

**Mini title: Nanoscale biophysics**  
**Title: Stretching the resolution limit of atomic force microscopy**

Bart W. Hoogenboom<sup>1,2</sup>

<sup>1</sup> London Centre for Nanotechnology, University College London, London WC1H 0AH, UK

<sup>2</sup> Department of Physics and Astronomy, University College London, WC1E 6BT London, UK

[b.hoogenboom@ucl.ac.uk](mailto:b.hoogenboom@ucl.ac.uk)

Atomic force microscopy (AFM) is unique in visualizing functional biomolecules in aqueous solution at ~1 nm resolution. By borrowing localization methods from fluorescence microscopy, AFM has been shown to discern structural domains that may be separated by only a few Ångströms.

---

In the early 2000s, Paul Selvin and colleagues employed fluorescence microscopy to determine how myosin V, a two-legged molecular motor, walks along actin fibres. This seemed a daunting task, since electron microscopy had shown that the maximum distance between the two legs was about 36 nm (Ref. <sup>1</sup>), which is an order or magnitude below the spatial resolution of fluorescence microscopy as set by the diffraction limit. However, by attaching a fluorophore to one of the motor legs and by determining the location of the corresponding fluorescent blob along the actin fibre, single-leg step sizes could be measured to within  $\pm 5$  nm uncertainty. These measurements demonstrated that myosin V walks “hand over hand” and illustrated that *localization accuracy* can be vastly superior to *resolution* in microscopy<sup>2</sup>. It took several more years to actually “see” the stepping of myosin V at nanometre resolution, requiring the use of AFM instead of fluorescence microscopy, in a study<sup>3</sup> that represents a hallmark of high-speed AFM. Writing in *Nature*, Heath *et al.*<sup>4</sup> now describe a method that applies localization algorithms from fluorescence microscopy to AFM, to localize and distinguish structural features of membrane proteins at sub-nanometre accuracy.

Historically, the appeal of AFM (and of its elder sibling scanning tunnelling microscopy) lies in the ability to resolve and hence “see” individual atoms at a sample surface. Since atomic resolution was robustly demonstrated in aqueous solution in the mid 2000s<sup>5,6</sup>, one might reasonably expect AFM to allow for atomic-resolution imaging of functional biomolecules “at work” under near-physiological conditions<sup>7</sup>. However, the lateral (*xy*) resolution on biological samples is still ~1 nm at best, with no significant improvement on that value since the results first obtained on two-dimensional lattices of membrane proteins in Andreas Engel’s lab in the mid-1990s<sup>8</sup>, notwithstanding occasional higher-resolution glimpses of specific structural domains on other biomolecules<sup>9,10</sup>. Contrasting with the huge advances made on reproducibility, versatility and temporal resolution of bio-AFM<sup>11</sup>, this lack of progress in spatial resolution is related to how the AFM probe (“tip”) traces the contours of a sample surface in a similar way as a blind person’s finger reads Braille, providing a three-dimensional (*xyz*) map of the surface topography.

In essence, the resolution of AFM is determined by the contact area between the AFM tip and the sample surface<sup>12</sup>, such that in principle, higher resolution can be obtained with sharper tips. Yet the tip-sample contact area may be increased and hence resolution degraded when the surface adheres to the tip (Fig. 1a). In addition, fluctuations of the underlying soft matter may confuse the detection of the sample by the tip (Fig. 1b), and so can dynamics of the molecules at the sample surface (Fig. 1c), resulting from intrinsic molecular fluctuations or from transient deformations due to the forces exerted by the AFM tip. Disregarding these effects, AFM images represent what is generally described as a convolution of the sample surface with the tip shape<sup>12</sup> (Fig. 1d), even though this is not a mathematical convolution *stricto sensu*<sup>13</sup>, such that power-spectrum analysis of AFM images may suggest an artefactual, overestimated resolution<sup>14</sup>. Given that AFM tips can be prepared to

about  $\sim 1$  nm tip radius, this convolution sets a rather hard limit to the spatial resolution, unless samples are atomically flat.

However, as is the case for fluorescence microscopy, the *resolution* limit does not preclude the *localization* of structural domains at a substantially higher *accuracy*, as already demonstrated for AFM by Simon Scheuring *et al.*<sup>15</sup> in 2002: Instead of mapping the local sample height ( $z$ ) as a function of lateral ( $xy$ ) position, one can detect local height maxima in the image and plot the distribution of relative peak ( $xy$ ) positions as acquired over multiple, suitable aligned molecules. The resulting peaking-probability maps could pinpoint the locations of protruding protein domains to an accuracy limited by the pixel size in the original data (see Ref. <sup>15</sup> and Fig. 2a,b, where this pixel size is  $2\sim 3$  Å).

In Heath *et al.*<sup>4</sup>, Scheuring's team have interpolated AFM data to a substantially finer pixel size and used the thus oversampled AFM images to improve peak-localization accuracy, very similar to procedures in localization microscopy as based on fluorescence images. The greyscale peaking-probability maps can also be complemented with a colour coding that represents the local height ( $z$ ) as recorded at the  $xy$  positions of the peaks. The result is a hybrid "localization AFM" (LAFM) map in which brightness refers to peaking-probability and in which an RGB colour scheme refers to the local height as measured in the original AFM topography (Fig. 2c).

As explained above, the effective resolution of a peaking-probability map can be substantially higher than spatial resolution in the microscopy image(s) on which it is based. The question is to what extent this allows to discern between different surface features. As demonstrated by LAFM results on membrane proteins<sup>4</sup>, peaking-probability maps allow the distinction between structural features that may be as close together as  $\sim 2$  Å, where such distinction remains hidden in the more coarsely pixelated peaking-probability maps based on the original, non-interpolated data.

LAFM has some elements in common with the super-resolution methods that have revolutionized fluorescence microscopy<sup>16–18</sup>. Those methods ensure that only a small sub-population of fluorophores emits light at a given time, such that isolated fluorophores can be localized at a much higher accuracy than is possible when they all emit light at the same time. A high-resolution image can then be reconstructed by summing localization maps that are recorded at different times. However, it remains to be established how well this principle translates to (L)AFM: unlike the light emitted by fluorophores in super-resolution microscopy, the tip-sample forces in AFM may not be as easily switched on and off for subsets of atoms at the surface. As proposed by Heath *et al.*<sup>4</sup>, the analogy may hold in cases where the dynamics of otherwise hidden atoms or structural domains is such that they can transiently protrude above neighbouring surface topography, and therewith be transiently detected by the AFM tip. Obviously, the plausibility of this scenario – and hence the potential benefits of LAFM – strongly depends on the local sample dynamics and corrugation.

The promise of LAFM lies in stretching a rather hard resolution limit of AFM on biological samples. At the same time, it raises intriguing questions about the origin and nature of the resolution as reported for the peaking-probability maps. Since the LAFM analysis code is now freely available<sup>4</sup>, there is ample scope for verifying its robustness and for its validation on a wider variety of samples.

## References

1. Walker, M. L., Burgess, S. A., Sellers, J. R., Wang, F., Iijima, J. A. H., Trinick, J. & Knight, P. J. Two-headed binding of a processive myosin to F-actin. *Nature* **405**, 1998–2001 (2000).
2. Yildiz, A., Forkey, J. N., McKinney, S. A., Ha, T., Goldman, Y. E. & Selvin, P. R. Myosin V Walks Hand-Over-Hand: Single Fluorophore Imaging with 1.5-nm Localization. *Science* **300**, 2061–2065 (2003).

3. Kodera, N., Yamamoto, D., Ishikawa, R. & Ando, T. Video imaging of walking myosin V by high-speed atomic force microscopy. *Nature* **468**, 72–6 (2010).
4. Heath, G. R., Kots, E., Robertson, J. L., Lansky, S., Khelashvili, G., Weinstein, H. & Scheuring, S. Localization atomic force microscopy. *Nature* **594**, 385–390 (2021).
5. Fukuma, T., Kobayashi, K., Matsushige, K. & Yamada, H. True atomic resolution in liquid by frequency-modulation atomic force microscopy. *Appl. Phys. Lett.* **87**, 034101 (2005).
6. Hoogenboom, B. W., Hug, H. J., Pellmont, Y., Martin, S., Frederix, P. L. T. M., Fotiadis, D. & Engel, A. Quantitative dynamic-mode scanning force microscopy in liquid. *Appl. Phys. Lett.* **88**, 193109 (2006).
7. Engel, A. & Müller, D. J. Observing single biomolecules at work with the atomic force microscope. *Nat. Struct. Biol.* **7**, 715–718 (2000).
8. Schabert, F. A. & Engel, A. Reproducible acquisition of Escherichia coli porin surface topographs by atomic force microscopy. *Biophys. J.* **67**, 2394–2403 (1994).
9. Asakawa, H., Ikegami, K., Setou, M., Watanabe, N., Tsukada, M. & Fukuma, T. Submolecular-scale imaging of  $\alpha$ -helices and C-terminal domains of tubulins by frequency modulation atomic force microscopy in liquid. *Biophys. J.* **101**, 1270–1276 (2011).
10. Ido, S., Kimura, K., Oyabu, N., Kobayashi, K., Tsukada, M., Matsushige, K. & Yamada, H. Beyond the helix pitch: Direct visualization of native DNA in aqueous solution. *ACS Nano* **7**, 1817–1822 (2013).
11. Dufrêne, Y. F., Ando, T., Garcia, R., Alsteens, D., Martinez-Martin, D., Engel, A., Gerber, C. & Müller, D. J. Imaging modes of atomic force microscopy for application in molecular and cell biology. *Nat. Nanotechnol.* **12**, 295–307 (2017).
12. Gan, Y. Atomic and subnanometer resolution in ambient conditions by atomic force microscopy. *Surf. Sci. Rep.* **64**, 99–121 (2009).
13. Odin, C., Aimé, J. P., Kaakour, Z. El & Bouhacina, T. Tip's finite size effects on atomic force microscopy in the contact mode: simple geometrical considerations for rapid estimation of apex radius and tip angle based on the study of polystyrene latex balls. *Surf. Sci.* **317**, 321–340 (1994).
14. Fechner, P., Boudier, T., Mangenot, S., Jaroslowski, S., Sturgis, J. N. & Scheuring, S. Structural Information, Resolution, and Noise in High-Resolution Atomic Force Microscopy Topographs. *Biophys. J.* **96**, 3822–3831 (2009).
15. Scheuring, S., Müller, D. J., Stahlberg, H., Engel, H. A. & Engel, A. Sampling the conformational space of membrane protein surfaces with the AFM. *Eur. Biophys. J.* **31**, 172–178 (2002).
16. Klar, T. A., Jakobs, S., Dyba, M., Egner, A. & Hell, S. W. Fluorescence microscopy with diffraction resolution barrier broken by stimulated emission. *Proc. Natl. Acad. Sci. U. S. A.* **97**, 8206–8210 (2000).
17. Betzig, E., Patterson, G. H., Sougrat, R., Lindwasser, O. W., Olenych, S., Bonifacino, J. S., Davidson, M. W., Lippincott-schwartz, J. & Hess, H. F. Imaging Intracellular Fluorescent Proteins at Nanometer Resolution. *Science* **313**, 1642–1646 (2006).
18. Rust, M. J., Bates, M. & Zhuang, X. Sub-diffraction-limit imaging by stochastic optical reconstruction microscopy (STORM). *Nat. Methods* **3**, 793–795 (2006).
19. Pyne, A., Thompson, R., Leung, C., Roy, D. & Hoogenboom, B. W. Single-molecule reconstruction of oligonucleotide secondary structure by atomic force microscopy. *Small* **10**, 3257–3261 (2014).
20. Scheuring, S., Ringler, P., Borgnia, M., Stahlberg, H., Müller, D. J., Agre, P. & Engel, A. High resolution AFM topographs of the Escherichia coli water channel aquaporin Z. *EMBO J.* **18**, 4981–4987 (1999).

### Competing Interests statement

The author declares no conflict of interest.

## Figure captions

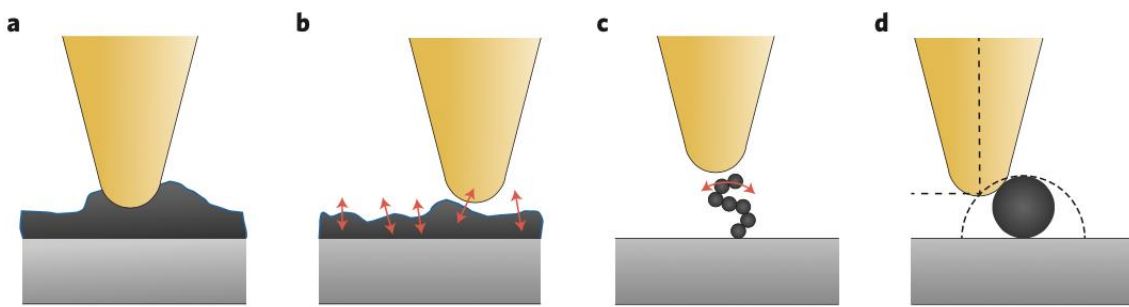


**Figure 1 | Factors that can limit spatial resolution in bio-AFM.** **a**, Sample (black) sticking to the AFM tip (orange) over larger area, increasing the tip-sample contact area. **b**, Unstable or dynamic substrate, confusing detection of the surface by the AFM tip. **c**, Mobility of the molecules at the surface, which can be intrinsic or induced by AFM tip, blurring the view obtained by AFM. **d**, In many cases, the AFM tip first contacts the sample sideways. Hence the lateral and vertical positions of the tip end (indicated by dashed lines) do not accurately reflect the position of the tip-sample contact, except for the most protruding parts of the sample. Since the AFM topography (dotted curve) refers to measurement of the tip position, this leads to a broadened representation of the sample surface<sup>19</sup>. Generally, this broadening reduces the overall resolution, although not the accuracy at which maxima in the surface topography (“peaks”) can be detected.

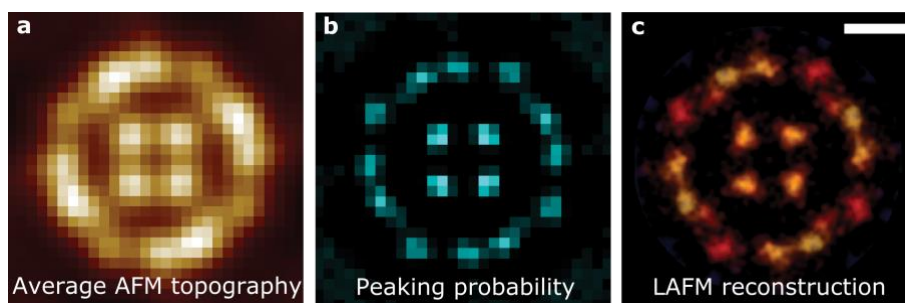


**Figure 2 | From peaks to peaking probability to LAFM.** **a**, AFM topography of aquaporin AqpZ, averaged over multiple molecules<sup>20</sup>, here recorded at a pixel resolution of 3.3 Å. **b**, Peaking probability map<sup>15</sup>, which represents the likelihood of detecting a local maximum as a function of relative (*xy*) position, as determined from the separate AFM images that yielded the average AFM topography in **a**. **c**, The LAFM reconstructions<sup>4</sup> are peaking probability maps obtained after data interpolation to a higher pixel density, in which brightness refers to peaking probability and a colour scale refers to the sample height detected at the corresponding *xy* positions. Scale bar: 20 Å. Figure adapted from Ref. <sup>4</sup>.